Rare-Earth Germanium Antimonides $RE_6Ge_{5-x}Sb_{11+x}$ (RE = La−Nd, Sm, Gd−Dy). I. Syntheses and Structures

Robert Lam, Robert McDonald,† and Arthur Mar*

Department of Chemistry, University of Alberta, Edmonton, Alberta, Canada T6G 2G2

Received August 17, 2000

The ternary rare-earth germanium antimonides $RE_6Ge_{5-x}Sb_{11+x}$ (RE = La−Nd, Sm, Gd−Dy) have been synthesized through direct reaction of the elements at 950 °C, and the structures of the representative members $La_6Ge_{2.8(1)}Sb_{13.2(1)}$ (a = 4.3034(8) Å, b = 10.851(3) Å, c = 27.073(7) Å), $Nd_6Ge_{3.6(1)}Sb_{12.4(1)}$ (a = 4.2310(3) Å, b = 10.6362(7) Å, c = 26.526(2) Å), and $Gd_6Ge_{4.3(1)}Sb_{11.7(1)}$ (a = 4.1509(3) Å, b = 10.4438(7) Å, c = 26.2400(18) Å) have been determined by single-crystal X-ray diffraction. They crystallize in the orthorhombic space group D_{2h}^{25}-*Immm* with Z = 2. The structures consist of columns of Sb-centered face-sharing RE_6 trigonal prisms aligned along [100], separated by interconnecting walls of Ge and Sb atoms. A wide array of Ge−Ge, Ge−Sb, and Sb−Sb interactions is found within these walls, ranging from strong covalent bonds to intermediate one-electron partial bonds to weak van der Waals forces.

Introduction

Our continuing exploration of the ternary rare-earth main-group-element antimonide systems $RE_xA_ySb_z$ (A = Al, Ga, In, Si, Ge, Sn) has revealed a strikingly rich and structurally diverse crystal chemistry, reinforced by recent discoveries of the novel compounds $La_{13}Ga_8Sb_{21}$,[1] $RE_{12}Ga_4Sb_{23}$ (RE = La−Nd, Sm),[1] $REIn_{1-x}Sb_2$ (RE = La−Nd),[2] $RESn_xSb_2$ (RE = La−Nd, Sm),[3] and $EuSn_3Sb_4$.[4] In all of these systems, the Zintl concept[5−8] is invoked as a tool to rationalize the complex networks formed by the electronegative main-group atoms and characterized by extensive homoatomic (Ga−Ga, In−In, Sn−Sn, Sb−Sb) bonding. Historically, the Zintl concept has served as a successful paradigm for explaining the bonding in valence compounds of the form M_xA_y or $M_xA_yB_z$ (M = alkali or alkaline-earth metal; A, B = main-group elements), where the assumption of complete transfer of valence electrons from the electropositive elements (M) to the electronegative main-group atoms (A, B), which use them to satisfy the octet rule, is tenable. However, the presence of "nonclassical" structural features such as one-dimensional Sb ribbons or two-dimensional Sb square sheets, weak homoatomic bonding of the main-group elements, and partial covalent character in bonds between rare-earth and main-group elements in the aforementioned ternary compounds poses challenging problems which test the limits of this important concept.[9] The exception is the compound $EuSn_3Sb_4$, whose structure is constructed from "classical" building blocks of trigonal pyramids of Sn and Sb and Sn-centered tetrahedra, for which the Zintl concept is applied in a straightforward manner.[4]

A recent investigation of the Ce−Ge−Sb ternary phase diagram[10] has revealed a potentially rich system, yielding three new ternary compounds: Ce_2GeSb_3 (superstructure of $ThGe_2$-type), "$Ce_5Ge_3Sb_2$" (unknown structure), and Ce_3GeSb (La_3GeIn-type). We report here the syntheses and properties of a new series of ternary rare-earth germanium antimonides, $RE_6Ge_{5-x}Sb_{11+x}$ (RE = La−Nd, Sm, Gd−Dy), and the structures of the representative members $La_6Ge_{2.8(1)}Sb_{13.2(1)}$, $Nd_6Ge_{3.6(1)}Sb_{12.4(1)}$, and $Gd_6Ge_{4.3(1)}Sb_{11.7(1)}$. Their complex structures feature columns of face-sharing trigonal prisms of rare-earth atoms, separated by interconnecting walls defined by Ge and Sb atoms. Interest in ternary rare-earth-containing compounds is derived from the presence of f electrons which may give rise to useful magnetic and electronic properties, while interactions among three elemental components introduce a level of complexity not accessible in binary systems. The electronic and magnetic properties of these materials are detailed separately.[11]

Experimental Section

Synthesis. Reactions of powders of the elements (La−Nd, 99.9%, Alfa-Aesar; Sm, Gd−Dy, 99.9%, Cerac; Ge, 99.999%, Cerac; Sb, 99.995%, Aldrich) were carried out on a 0.25 g scale in evacuated fused-silica tubes (8 cm length; 10 mm i.d.). Elemental compositions of selected crystals were determined by calibrated EDX (energy-dispersive X-ray) analysis on a Hitachi S-2700 scanning electron microscope (Table 1). X-ray powder patterns were obtained on an Enraf-Nonius FR552 Guinier camera (Cu $K\alpha_1$ radiation; Si standard) and analyzed with the Filmscan and Jade 3.1 software packages.[12]

Single crystals of $La_6Ge_{2.8(1)}Sb_{13.2(1)}$, $Nd_6Ge_{3.6(1)}Sb_{12.4(1)}$, and $Gd_6Ge_{4.3(1)}Sb_{11.7(1)}$ used in the structure determination were obtained from reactions of the corresponding rare-earth element, Ge, and Sb in the ratio 6:5:11. The samples were heated to 570 °C for 1 day and then at

* To whom correspondence should be addressed. Telephone: (780) 492−5592. Fax: (780) 492−8231. E-mail: arthur.mar@ualberta.ca.
† Faculty Service Officer, Structure Determination Laboratory.

(1) Mills, A. M.; Mar, A. *Inorg. Chem.* **2000**, *39*, 4599.
(2) Ferguson, M. J.; Ellenwood, R. E.; Mar, A. *Inorg. Chem.* **1999**, *38*, 4503.
(3) Ferguson, M. J.; Hushagen, R. W.; Mar, A. *Inorg. Chem.* **1996**, *35*, 4505.
(4) Lam, R.; Zhang, J.; Mar, A. *J. Solid State Chem.* **2000**, *150*, 371.
(5) *Chemistry, Structure, and Bonding of Zintl Phases and Ions*; Kauzlarich, S. M., Ed.; VCH: New York, 1996, and references therein.
(6) Schäfer, H. *Annu. Rev. Mater. Sci.* **1985**, *15*, 1.
(7) Corbett, J. D. *Chem. Rev.* **1985**, *85*, 383.
(8) von Schnering, H. G. *Angew. Chem., Int. Ed. Engl.* **1981**, *20*, 33.
(9) Papoian, G. A.; Hoffmann, R. *Angew. Chem., Int. Ed. Engl.* **2000**, *39*, 2408.
(10) Steskiv, A. O.; Pavlyuk, V. V.; Bodak, O. I. *Pol. J. Chem.* **1998**, *72*, 956.
(11) Deakin, L.; Lam, R.; Mar, A. *Inorg. Chem.* **2001**, *40*, 960.
(12) Filmscan and Jade 3.1; Materials Data Inc., Livermore, CA, 1996.

10.1021/ic0009472 CCC: $20.00
Published on Web 01/27/2001

Table 1. Elemental (EDX) Analyses for Compounds $RE_6Ge_{5-x}Sb_{11+x}$ (RE = La−Nd, Sm, Gd−Dy)

compd	amt (mol %)			no. of samples
	RE	Ge	Sb	
$La_6Ge_{2.8(1)}Sb_{13.2(1)}$[a]	28.7(1)	11.7(2)	59.5(3)	2
(calcd[a]	27	13	60)	
$Ce_6Ge_{5-x}Sb_{11+x}$	29.2(6)	16(1)	54.6(6)	5
$Pr_6Ge_{5-x}Sb_{11+x}$	30.6(6)	16.6(8)	52.8(4)	5
$Nd_6Ge_{3.6(1)}Sb_{12.4(1)}$[a]	27.6(6)	16(1)	55.9(4)	3
(calcd[a]	27	16	56)	
$Sm_6Ge_{5-x}Sb_{11+x}$	29.1(1)	17.3(6)	53.6(5)	2
$Gd_6Ge_{4.3(1)}Sb_{11.7(1)}$[a]	27.7(6)	19.7(1)	52.6(5)	2
(calcd[a]	27	20	53)	
$Tb_6Ge_{5-x}Sb_{11+x}$	32.2(2)	20.8(8)	47.0(6)	4
$Dy_6Ge_{5-x}Sb_{11+x}$	29.3(4)	16.8(6)	53.9(5)	6

[a] These formulas represent compositions deduced from refinements of the crystal structures.

Table 2. Cell Parameters for the Compounds $RE_6Ge_{5-x}Sb_{11+x}$ (RE = La−Nd, Sm, Gd−Dy)

compd	*a* (Å)	*b* (Å)	*c* (Å)	*V* (Å^3)
$La_6Ge_{2.8(1)}Sb_{13.2(1)}$	4.3289(7)	10.857(1)	27.076(3)	1272.6(2)
$Ce_6Ge_{5-x}Sb_{11+x}$	4.2972(7)	10.740(1)	26.791(4)	1236.4(2)
$Pr_6Ge_{5-x}Sb_{11+x}$	4.2674(9)	10.677(2)	26.626(5)	1213.1(3)
$Nd_6Ge_{3.6(1)}Sb_{12.4(1)}$	4.2412(8)	10.637(2)	26.552(4)	1197.8(3)
$Sm_6Ge_{5-x}Sb_{11+x}$	4.1942(7)	10.537(1)	26.350(3)	1164.5(2)
$Gd_6Ge_{4.3(1)}Sb_{11.7(1)}$	4.1511(6)	10.440(1)	26.228(3)	1136.7(2)
$Tb_6Ge_{5-x}Sb_{11+x}$	4.1305(8)	10.393(2)	26.139(4)	1122.1(2)
$Dy_6Ge_{5-x}Sb_{11+x}$	4.1032(10)	10.345(2)	26.014(5)	1104.2(3)

950 °C for 2 days, cooled to 500 °C over 1 day, and finally cooled to 20 °C over 5 h. The extent of rare-earth substitution was investigated, and in total, eight members in this series $RE_6Ge_{5-x}Sb_{11+x}$ (RE = La−Nd, Sm, Gd−Dy) could be successfully prepared. The products typically consisted of aggregates of shiny gray bulky needle-shaped crystals of $RE_6Ge_{5-x}Sb_{11+x}$ and gray powder, containing mostly the ternary compound and unreacted Ge. Unlike the other reactions which produced large quantities of single crystals, the Dy−Ge−Sb reaction resulted in only a few tiny needle-shaped crystals of the ternary compound or the binary phase DySb[13] and reddish brown powder consisting of DySb (major phase) and $Dy_6Ge_{5-x}Sb_{11+x}$, as well as unreacted Ge. Attempts to substitute other trivalent rare-earth metals beyond Dy were unsuccessful, resulting instead in a mixture of the binary phase *RE*Sb (major phase), unreacted Ge, and other unidentified phases. Substitutions involving the divalent Eu and Yb metals resulted predominantly in the binary phases $EuSb_2$[14] and $YbSb_2$,[15] respectively, in addition to unreacted Ge and other unidentified phases. The powder patterns of the entire series $RE_6Ge_{5-x}Sb_{11+x}$ (RE = La−Nd, Sm, Gd−Dy) were indexed, and the cell parameters refined by least-squares fits with the use of the program POLSQ[16] are given in Table 2. The observed and calculated interplanar distances, as well as intensities determined using the program LAZY-PULVERIX,[17] are listed in Tables S1−S8 (Supporting Information).

Structure Determination. X-ray structure determinations were performed on representative members in the series $RE_6Ge_{5-x}Sb_{11+x}$ (RE = La−Nd, Sm, Gd−Dy), one each for the early, middle, and late rare-earth substitutions. Preliminary cell parameters for $La_6Ge_{2.8(1)}Sb_{13.2(1)}$, $Nd_6Ge_{3.6(1)}Sb_{12.4(1)}$, and $Gd_6Ge_{4.3(1)}Sb_{11.7(1)}$ were determined from Weissenberg photographs, which revealed Laue symmetry *mmm* and systematic extinctions (*hkl*: $h + k + l = 2n + 1$) consistent with the orthorhombic space groups *Immm*, *Imm*2, *I*222, and $I2_12_12_1$. Final cell parameters for all three compounds were obtained from least-squares analyses of the setting angles of 24 reflections centered on an Enraf-Nonius CAD4 diffractometer. Intensity data were collected at 22 °C with the $\theta-2\theta$ scan technique in the range $3° \le 2\theta(\text{Mo K}\alpha) \le 70°$. Crystal data and further details of the data collection are given in Table 3. All calculations were carried out with the use of the SHELXTL (version 5.1) package.[18] Conventional atomic scattering factors and anomalous dispersion corrections were used.[19] The intensity data were processed and corrected for absorption by a semiempirical method based on ψ-scans in XPREP. Initial atomic positions were found by direct methods using XS followed by subsequent difference Fourier syntheses, and refinements were performed by least-squares methods using XL.

Table 3. Crystallographic Data for $RE_6Ge_{5-x}Sb_{11+x}$ (RE = La, Nd, Gd)

	$La_6Ge_{2.8(1)}$-$Sb_{13.2(1)}$	$Nd_6Ge_{3.6(1)}$-$Sb_{12.4(1)}$	$Gd_6Ge_{4.3(1)}$-$Sb_{11.7(1)}$
formula mass (amu)	2643.81	2636.46	2678.27
space group	D_{2h}^{25}-*Immm* (No. 71)	D_{2h}^{25}-*Immm* (No. 71)	D_{2h}^{25}-*Immm* (No. 71)
a (Å)[a]	4.3034(8)	4.2310(3)	4.1509(3)
b (Å)[a]	10.851(3)	10.6362(7)	10.4438(7)
c (Å)[a]	27.073(7)	26.526(2)	26.2400(18)
V (Å^3)	1264.2(5)	1193.73(15)	1137.53(14)
Z	2	2	2
T (°C)	22	22	22
λ (Å)	0.710 73	0.710 73	0.710 73
ρ_{calcd} (g cm^{-3})	6.945	7.335	7.819
μ(Mo Kα) (cm^{-1})	269.6	309.7	363.9
$R(F)$ for $F_o^2 > 2\sigma(F_o^2)$[b]	0.041	0.031	0.042
$R_w(F_o^2)$[c]	0.098	0.068	0.101

[a] Obtained from a refinement constrained so that $\alpha = \beta = \gamma = 90°$. [b] $R(F) = \sum||F_o| - |F_c||/\sum|F_o|$. [c] $R_w(F_o^2) = [\sum[w(F_o^2 - F_c^2)^2]/\sum wF_c^4]^{1/2}$; $w^{-1} = [\sigma^2(F_o^2) + (Ap)^2 + Bp]$, where $p = [\max(F_o^2,0) + 2F_c^2]/3$. A = 0.0513, 0.0298, and 0.0471 and B = 3.3625, 1.2302, and 0 for $La_6Ge_{2.8(1)}Sb_{13.2(1)}$, $Nd_6Ge_{3.6(1)}Sb_{12.4(1)}$, and $Gd_6Ge_{4.3(1)}Sb_{11.7(1)}$, respectively.

For $La_6Ge_{2.8(1)}Sb_{13.2(1)}$, the centrosymmetric space group *Immm* was chosen on the basis of intensity statistics and the successful structure solution. Once all atomic positions were found, a refinement based on the formula "$La_6Ge_5Sb_{11}$" revealed considerable electron density ($\Delta\rho_{max}$ = 73.91, $\Delta\rho_{min}$ = −23.36 e Å^{-3}) at the site (~0.4, $^1/_2$, 0), located 0.44 Å from Sb(4) ($^1/_2$, $^1/_2$, 0). Reminiscent of the "sliding distortion" observed for the central atom of similar Sb ribbons previously encountered in the related compound La_6MnSb_{15},[20,21] Sb(4) was subsequently reassigned exclusively to the new site (~0.4, $^1/_2$, 0). Shifting Sb(4) off the $^1/_2$ *x y* mirror plane resulted in significantly improved agreement factors, but more importantly, the original site ($^1/_2$, $^1/_2$, 0) did not reappear in the difference Fourier map in later refinements. However, close Sb(4)−Sb(4) contacts (0.60 Å) required the occupancy of Sb(4) to be fixed at the theoretical maximum of 50% (51.4(3)% if allowed to refine). The sites at (0, ~0.12, ~0.15) (M(1)) and (0, ~0.04, 0) (M(2)) were next assumed to be occupied only by Ge, since reasonable Ge−Ge and Ge−Sb distances were obtained. This ordered model corresponds to the ideal formulation "$La_6Ge_5Sb_{11}$" (Anal. Calcd: La, 27; Ge, 23; Sb, 50). However, given the consistently higher percentage of Sb and lower percentage of Ge observed in the EDX analyses (Table 1) relative to the current formula, the possibility that the sites M(1) and M(2) are occupied by a mixture of Ge and Sb was explored. The presence of residual electron density near these two sites and their relatively low displacement parameters, as well as chemical arguments to be presented later, provided convincing evidence in favor of a disordered model. The occupancy of M(1) was assumed to be 100% (121(1)% when refined with M(1) = Ge), and that for M(2)

(13) Lévy, F. *Phys. Kondens. Mater*. **1969**, *10*, 85.
(14) Hulliger, F.; Schmelczer, R. *J. Solid State Chem*. **1978**, *26*, 389.
(15) Wang, R.; Bodnar, R.; Steinfink, H. *Inorg. Chem*. **1966**, *5*, 1468.
(16) POLSQ: Program for least-squares unit cell refinement. Modified by D. Cahen and D. Keszler, Northwestern University, 1983.
(17) Yvon, K.; Jeitschko, W.; Parthé, E. *J. Appl. Crystallogr*. **1977**, *10*, 73.
(18) Sheldrick, G. M. SHELXTL, version 5.1; Bruker Analytical X-ray Systems, Inc., Madison, WI, 1997.
(19) *International Tables for X-ray Crystallography*; Wilson, A. J. C., Ed.; Kluwer: Dordrecht, The Netherlands, 1992; Vol. C.
(20) Sologub, O.; Vybornov, M.; Rogl, P.; Hiebl, K.; Cordier, G.; Woll, P. *J. Solid State Chem*. **1996**, *122*, 266.
(21) Papoian, G.; Hoffmann, R. *J. Solid State Chem*. **1998**, *139*, 8.

was assumed to be 50% (65(1)% when refined with M(2) = Ge) owing to close M(2)−M(2) contacts (0.85 Å) as a result of the *x* 0 *z* mirror plane. Successive refinements in which the sites M(1) and M(2) were constrained to be fully occupied and half-occupied, respectively, by a mixture of Ge and Sb resulted in occupancies of 61(3)% Ge(1) and 39(2)% Sb(6) in the site (0, ∼0.12, ∼0.15) and 19(2)% Ge(2) and 31-(1)% Sb(7) in the site (0, ∼0.04, 0). These refinements also led to reasonable values for the anisotropic displacement parameters, a featureless difference electron density map ($\Delta\rho_{max}$ = 4.82, $\Delta\rho_{min}$ = −5.36 e Å^{-3}), and overall improvements in the agreement factors. A series of refinements allowing the occupancies of successive atoms to vary freely revealed full occupancies (99.4(4)−100.1(4)%) for all other atoms. The final refined formula, $La_6Ge_{2.8(1)}Sb_{13.2(1)}$ (*Z* = 2) (Anal. Calcd: La, 27; Ge, 13; Sb, 60), is in excellent agreement with the elemental analysis.

The treatment of $Nd_6Ge_{3.6(1)}Sb_{12.4(1)}$ and $Gd_6Ge_{4.3(1)}Sb_{11.7(1)}$ proceeded similarly, given the resemblance of their intensity patterns to that of $La_6Ge_{2.8(1)}Sb_{13.2(1)}$. In both cases, the chosen space group *Immm* was further supported by the intensity statistics and the successful structure solutions. Atomic assignments were made using the structure of $La_6Ge_{2.8(1)}Sb_{13.2(1)}$ as an initial model. For $Nd_6Ge_{3.6(1)}Sb_{12.4(1)}$, moving Sb-(4) off the $^1/_2$ *x y* mirror plane to the position (∼0.44, $^1/_2$, 0) alleviated the problem of an elongated anisotropic displacement parameter (U_{11} = 0.124(4)) and resulted in the same solution as $La_6Ge_{2.8(1)}Sb_{13.2(1)}$. Analogous to the latter, occupancies of the M(2) (0, ∼0.04, 0) and Sb(4) sites were assumed to be at the maximum allowed limit of 50%, given the close distances to their crystallographic equivalents (M(2)−M(2) = 0.82 Å; Sb(4)−Sb(4) = 0.53 Å). Applying the Ge/Sb disorder model resulted in occupancies of 72(3)% Ge(1) and 28(2)% Sb(6) (M(1) site) and 36(2)% Ge(2) and 14(1)% Sb(7) (M(2) site). More importantly, however, these refinements also led to reasonable values for the anisotropic displacement parameters, a featureless difference electron density map ($\Delta\rho_{max}$ = 2.22, $\Delta\rho_{min}$ = −2.62 e Å^{-3}), and substantial improvements in the agreement factors. For $Gd_6Ge_{4.3(1)}Sb_{11.7(1)}$, structure refinements proceeded accordingly with only a few exceptions. Sb(4) was not displaced from the $^1/_2$ *x y* mirror plane but was successfully refined at the site ($^1/_2$, $^1/_2$, 0). The thermal ellipsoid of this site is slightly elongated along *a*, suggesting that a similar but less pronounced "sliding distortion" of the central Sb(4) atom may also be occurring in $Gd_6Ge_{4.3(1)}Sb_{11.7(1)}$, randomly displacing the atom slightly above and below the mirror plane but not sufficiently to render a split site. The other possible split site (0, ∼0.02, 0), analogous to position "M(2)" in the other compounds, remained situated away from the *x* 0 *z* mirror plane and also resulted in extremely short contacts (0.48 Å). Allowing the site to be occupied (50%) by a mixture of Ge and Sb revealed that the site was exclusively occupied by Ge. On the other hand, disorder still exists for the M(1) site with atomic distributions of 83(3)% Ge(1) and 17(2)% Sb(6). The final difference electron density map is featureless ($\Delta\rho_{max}$ = 3.74, $\Delta\rho_{min}$ = −4.93 e Å^{-3}). The occupancies of all other atoms in $Nd_6Ge_{3.6(1)}Sb_{12.4(1)}$ and $Gd_6Ge_{4.3(1)}Sb_{11.7(1)}$ were confirmed to be essentially 100% (95.7(6) −101.2(9)%) through independent refinements of their occupancies. Final refinements resulted in the formulations $Nd_6Ge_{3.6(1)}Sb_{12.4(1)}$ (*Z* = 2) (Anal. Calcd: Nd, 27; Ge, 16; Sb, 56) and $Gd_6Ge_{4.3(1)}Sb_{11.7(1)}$ (*Z* = 2) (Anal. Calcd: Gd, 27; Ge, 20, Sb, 53), which are in exceptionally good agreement with EDX analyses (Table 1).

There was initial concern over the chosen space group *Immm* because the related structure La_6MnSb_{15} was successfully solved in the lower symmetry space group *Imm*2 by removal of the mirror plane perpendicular to the *c* axis.[20] This had the effect of splitting the position 4*j* occupied by Sb(6) in that structure into two independent sites, 2*a* and 2*b*, of which only one was occupied, thereby eliminating the occurrence of extremely short Sb(6)−Sb(6) distances arising from the operation of the *x y* 0 mirror plane in the higher symmetry space group *Immm*. Two such positions, 4*f* (*x*, $^1/_2$, 0) and 4*g* (0, *y*, 0), exist in $RE_6Ge_{5-x}Sb_{11+x}$ (*Immm*) which also give rise to short interatomic contacts. Attempted solution of the structure in *I*2*mm* (removing the $^1/_2$ *x y* mirror plane), *Im*2*m* (removing the *x* 0 *z* mirror plane), or *I*222 (removing all mirror planes) was unsuccessful, as electron density was found in the two emerging split sites (e.g., ∼90 e Å^{-3} corresponding to the M(2) sites for the refinement in *Im*2*m*). The resulting Flack parameter[22] (e.g., 0.45-(6) for the refinement in *Im*2*m*) did not suggest the presence of an absolute structure, and further analysis of the final refined structure by ADDSYM[23] in the PLATON suite of programs,[24] which indicated the presence of mirror planes perpendicular to all 2-fold axes in the lower symmetry space groups, confirmed the positional disorder at these two sites. In the absence of a detectable superstructure, we opted for the higher symmetry space group *Immm* for the title compounds.

Table 4. Positional and Equivalent Isotropic Displacement Parameters for $RE_6Ge_{5-x}Sb_{11+x}$ (*RE* = La, Nd, Gd)

atom	Wyckoff position	*x*	*y*	*z*	U_{eq} (Å^2)[a]
			$La_6Ge_{2.8(1)}Sb_{13.2(1)}$		
La(1)	4*i*	0	0	0.26676(2)	0.01330(12)
La(2)	8*l*	0	0.19435(3)	0.405447(15)	0.01409(11)
Sb(1)	4*j*	$^1/_2$	0	0.35768(2)	0.01454(14)
Sb(2)	8*l*	0	0.30555(4)	0.288629(19)	0.01691(12)
Sb(3)	4*g*	0	0.29207(7)	0	0.01696(14)
Sb(4)[b]	4*f*	0.4300(3)	$^1/_2$	0	0.0162(3)
Sb(5)	4*j*	$^1/_2$	0	0.07187(3)	0.02475(17)
M(1)[c]	8*l*	0	0.12051(7)	0.14765(2)	0.0194(2)
M(2)[d]	4*g*	0	0.03926(17)	0	0.0216(5)
			$Nd_6Ge_{3.6(1)}Sb_{12.4(1)}$		
Nd(1)	4*i*	0	0	0.265928(19)	0.01241(10)
Nd(2)	8*l*	0	0.19331(3)	0.405129(14)	0.01321(9)
Sb(1)	4*j*	$^1/_2$	0	0.35698(2)	0.01363(12)
Sb(2)	8*l*	0	0.30521(4)	0.289096(18)	0.01542(10)
Sb(3)	4*g*	0	0.28797(7)	0	0.01682(13)
Sb(4)[b]	4*f*	0.4375(3)	$^1/_2$	0	0.0154(3)
Sb(5)	4*j*	$^1/_2$	0	0.06994(3)	0.02311(15)
M(1)[c]	8*l*	0	0.12165(6)	0.14609(3)	0.0169(2)
M(2)[d]	4*g*	0	0.0385(2)	0	0.0219(6)
			$Gd_6Ge_{4.3(1)}Sb_{11.7(1)}$		
Gd(1)	4*i*	0	0	0.26538(3)	0.01210(15)
Gd(2)	8*l*	0	0.19247(5)	0.40424(2)	0.01323(13)
Sb(1)	4*j*	$^1/_2$	0	0.35643(4)	0.01287(19)
Sb(2)	8*l*	0	0.30521(7)	0.28967(3)	0.01412(15)
Sb(3)	4*g*	0	0.28235(11)	0	0.0154(2)
Sb(4)	2*c*	$^1/_2$	$^1/_2$	0	0.0232(3)
Sb(5)	4*j*	$^1/_2$	0	0.06994(5)	0.0231(2)
M(1)[c]	8*l*	0	0.12196(11)	0.14510(4)	0.0159(4)
Ge(2)[d]	4*g*	0	0.0230(5)	0	0.0247(14)

[a] U_{eq} is defined as one-third of the trace of the orthogonalized $\mathbf{U}_{ij}$ tensor. [b] Occupancy fixed at 50%. [c] Site M(1) contains 61(3)% Ge(1) and 39(2)% Sb(6) in $La_6Ge_{2.8(1)}Sb_{13.2(1)}$, 72(3)% Ge(1) and 28(2)% Sb(6) in $Nd_6Ge_{3.6(1)}Sb_{12.4(1)}$, and 83(3)% Ge(1) and 17(2)% Sb(6) in $Gd_6Ge_{4.3(1)}Sb_{11.7(1)}$. [d] Site M(2) contains 19(2)% Ge(2) and 31(1)% Sb(7) in $La_6Ge_{2.8(1)}Sb_{13.2(1)}$; 36(2)% Ge(2) and 14(1)% Sb(7) in $Nd_6Ge_{3.6(1)}Sb_{12.4(1)}$, and 50% Ge(2) in $Gd_6Ge_{4.3(1)}Sb_{11.7(1)}$. *The remaining 50% represent vacancies*.

The atomic positions of $La_6Ge_{2.8(1)}Sb_{13.2(1)}$, $Nd_6Ge_{3.6(1)}Sb_{12.4(1)}$, and $Gd_6Ge_{4.3(1)}Sb_{11.7(1)}$ were standardized with the program STRUCTURE TIDY.[25] The final cycle of least-squares refinement on F_o^2 included anisotropic displacement parameters for all atoms and an isotropic extinction parameter. Final values of the positional and displacement parameters are given in Table 4. Selected interatomic distances are listed in Table 5. Further data (powder X-ray diffraction data, anisotropic displacement parameters, bond angles, and CIF files) are available as Supporting Information, and final structural amplitudes are available from A.M.

Results and Discussion

Trends. Elemental analyses on selected crystals of $RE_6Ge_{5-x}Sb_{11+x}$ (*RE* = La−Nd, Sm, Gd−Dy) (Table 1) show

(22) Flack, H. D. *Acta Crystallogr., Sect. A: Found. Crystallogr.* **1983**, *39*, 876.
(23) Le Page, Y. *J. Appl. Crystallogr.* **1988**, *21*, 983.
(24) Spek, A. L. PLATON, Version 281097; Utrecht University: Utrecht, The Netherlands, 1997.
(25) Gelato, L. M.; Parthé, E. *J. Appl. Crystallogr.* **1987**, *20*, 139.

Table 5. Selected Interatomic Distances (Å) in $RE_6Ge_{5-x}Sb_{11+x}$ (*RE* = La, Nd, Gd)

	$La_6Ge_{2.8(1)}Sb_{13.2(1)}$	$Nd_6Ge_{3.6(1)}Sb_{12.4(1)}$	$Gd_6Ge_{4.3(1)}Sb_{11.7(1)}$
RE(1)−*RE*(2) (×2)	4.3064(9)	4.2263(6)	4.1614(8)
RE(2)−*RE*(2)	4.2178(9)	4.1122(6)	4.0202(8)
RE(1)−Sb(1) (×2)	3.2694(8)	3.2107(6)	3.1647(9)
RE(1)−Sb(2) (×2)	3.3680(10)	3.3039(5)	3.2507(7)
RE(1)−Sb(2) (×4)	3.3661(6)	3.3012(4)	3.2455(6)
RE(1)−M(1)[a] (×2)	3.4797(11)	3.4321(9)	3.4035(13)
RE(2)−Sb(1) (×2)	3.2787(6)	3.2147(4)	3.1498(6)
RE(2)−Sb(2)	3.3850(10)	3.3000(6)	3.2285(9)
RE(2)−Sb(3) (×2)	3.3473(6)	3.2936(3)	3.2697(4)
RE(2)−Sb(4)	3.3303(7)	3.2605(4)	3.2179(5)
RE(2)−Sb(5)	3.3730(9)	3.3283(4)	3.2826(6)
RE(2)−M(1)[a] (×2)	3.2759(7)	3.1929(6)	3.1209(9)
Sb(2)−Sb(2) (×2)	3.2339(9)	3.1870(7)	3.1579(11)
Sb(2)−M(1)[a] (×2)	2.8722(7)	2.8348(6)	2.7956(9)
Sb(3)−Sb(4)	2.9179(11)	2.9175(9)	3.0780(8)
Sb(3)−Sb(4)	3.3328(11)	3.2788(10)	
Sb(3)−M(2)[b]	2.743(2)	2.653(2)	
Sb(3)−Ge(2)[b]			2.709(5)
Sb(5)-*M*(1)[a] (×4)	3.2480(9)	3.1985(7)	3.1337(12)
Sb(5)-*M*(2)[b] (×2)	2.9320(8)	2.8434(6)	
Sb(5)−Ge(2)[b] (×2)			2.7808(10)
M(1)−M(1)[a]	2.6154(16)	2.5879(14)	2.547(2)

[a] Site M(1) contains 61(3)% Ge(1) and 39(2)% Sb(6) in $La_6Ge_{2.8(1)}Sb_{13.2(1)}$, 72(3)% Ge(1) and 28(2)% Sb(6) in $Nd_6Ge_{3.6(1)}Sb_{12.4(1)}$, and 83(3)% Ge(1) and 17(2)% Sb(6) in $Gd_6Ge_{4.3(1)}Sb_{11.7(1)}$. [b] Site M(2) contains 19(2)% Ge(2) and 31(1)% Sb(7) in $La_6Ge_{2.8(1)}Sb_{13.2(1)}$, 36(2)% Ge(2) and 14(1)% Sb(7) in $Nd_6Ge_{3.6(1)}Sb_{12.4(1)}$, and 50% Ge(2) in $Gd_6Ge_{4.3(1)}Sb_{11.7(1)}$. *The remaining 50% represent vacancies*.

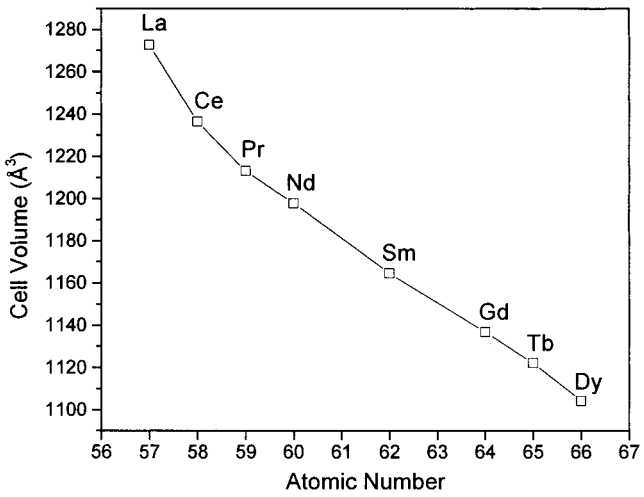

Figure 1. Plot of unit cell volume for $RE_6Ge_{5-x}Sb_{11+x}$ compounds. The lines are drawn only for guidance.

a gradual trend (mol %), as substitution proceeds across the series from La to Dy, of increasing Ge content coupled with a corresponding decrease in Sb while the amount of the *RE* component remains relatively constant. Although the quality of the elemental analyses greatly depends on the accuracy of the calibration standards of the elements, chemical arguments and results of the crystal structures of the early, intermediate, and late members also support the inverse proportionality of the Ge and Sb content in this series of compounds. Consistent with the lanthanide contraction and an oxidation state assignment of +3 for all *RE* atoms, the cell parameters (Figure 1, Table 2) show a monotonic decrease in all unit cell axes, as expected, given the three-dimensional nature of the structure.

Description of the Structures. A view of the structure of $La_6Ge_{2.8(1)}Sb_{13.2(1)}$ down the *a* axis is given in Figure 2, which shows the labeling scheme. Positions M(1) and M(2) represent

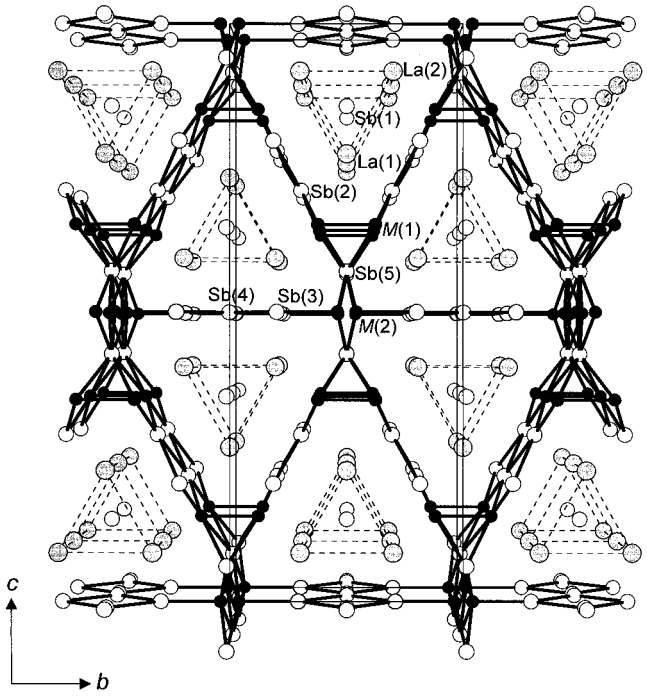

Figure 2. View of $La_6Ge_{2.8(1)}Sb_{13.2(1)}$ down the *a* axis showing the unit cell outline and the labeling scheme. The large lightly shaded circles are La atoms, the small solid circles are disordered sites (M(1) and M(2)) containing Ge and Sb, and the medium-sized open circles are Sb atoms. The dashed lines merely outline the assemblies of La_6 trigonal prisms.

disordered sites containing 61(3)% Ge(1), 39(2)% Sb(6) and 19(2)% Ge(2), 31(1)% Sb(7), respectively. (The remaining 50% in M(2) represent vacancies.) $Nd_6Ge_{3.6(1)}Sb_{12.4(1)}$ and $Gd_6Ge_{4.3(1)}Sb_{11.7(1)}$ are isostructural with $La_6Ge_{2.8(1)}Sb_{13.2(1)}$, differing only in the proportions of Ge and Sb at these two sites. As indicated previously, the Ge:Sb ratio increases as size of *RE* decreases, resulting in distributions of M(1) = 72(3)% Ge(1), 28(2)% Sb(6) and M(2) = 36(2)% Ge(2), 14(1)% Sb(7) for $Nd_6Ge_{3.6(1)}Sb_{12.4(1)}$ and M(1) = 83(3)% Ge(1), 17(2)% Sb(6) and M(2) = 50% Ge(2) for $Gd_6Ge_{4.3(1)}Sb_{11.7(1)}$. $RE_6Ge_{5-x}Sb_{11+x}$ adopts a new structure type, conveniently described as comprising Sb(1)-centered trigonal prisms, whose vertexes are the *RE*(1) and *RE*(2) atoms, which share triangular faces to form columns running along [100]. These columns are separated from each other by an intricate network of interconnecting walls defined by Ge and Sb atoms.

Although the structure is three-dimensional in character, it will be instructive to employ a "retrotheoretical" approach[21] to decompose it into lower dimensional subunits which can then be discussed more coherently. When the individual components are reassembled in an *aufbau* fashion later, insight can be gained on the overall complex structure. We begin by removing the electropositive *RE* atoms, revealing the underlying three-dimensional metalloid framework (Figure 3a). For clarity, position M(1) will be momentarily considered to be filled exclusively by Sb atoms. Next, the closely spaced disordered position M(2) is removed to generate a collection of three separated constituents (Figure 3b): linear arrays of essentially isolated Sb(1) atoms (0D), three-atom-wide Sb ribbons (1D), and kinked Sb square sheets (2D). The latter may be imagined to be derived from an idealized flat Sb square net by a process of folding at every fifth atom (Sb(5)).[21] The extracted components are represented schematically in Figure 3c.

A view of the one-dimensional three-atom-wide Sb ribbons (Sb(3)−Sb(4)−Sb(3)) which extend along [100] is shown in

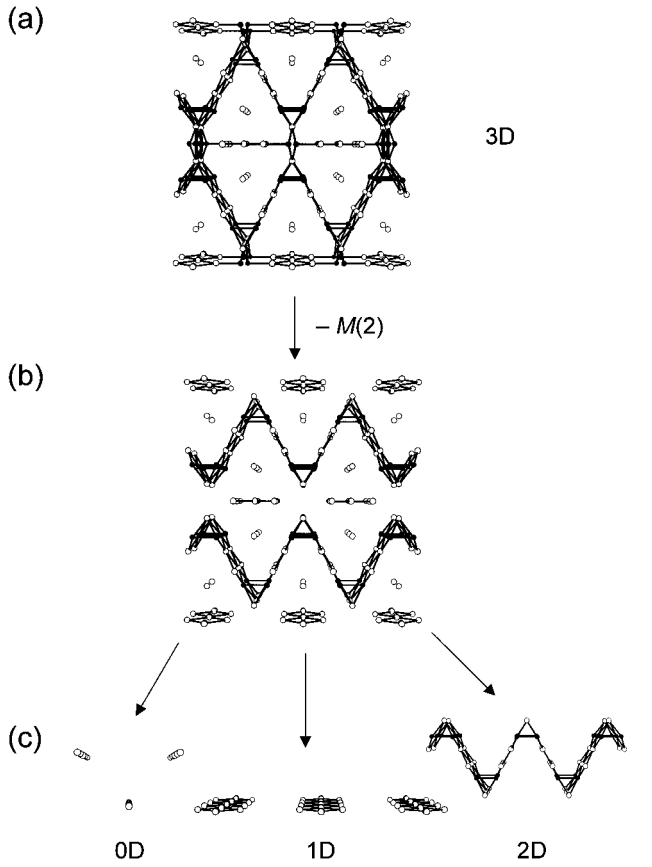

Figure 3. Schematic diagram illustrating the process of "retrotheoretical analysis" of the $RE_6Ge_{5-x}Sb_{11+x}$ structure, an artificial decomposition of (a) the complex three-dimensional anionic network, by means of (b) removing the M(2) atoms, into (c) discrete subunits of lower dimensionality (isolated Sb atoms, three-atom-wide Sb ribbons, and kinked Sb square sheets).

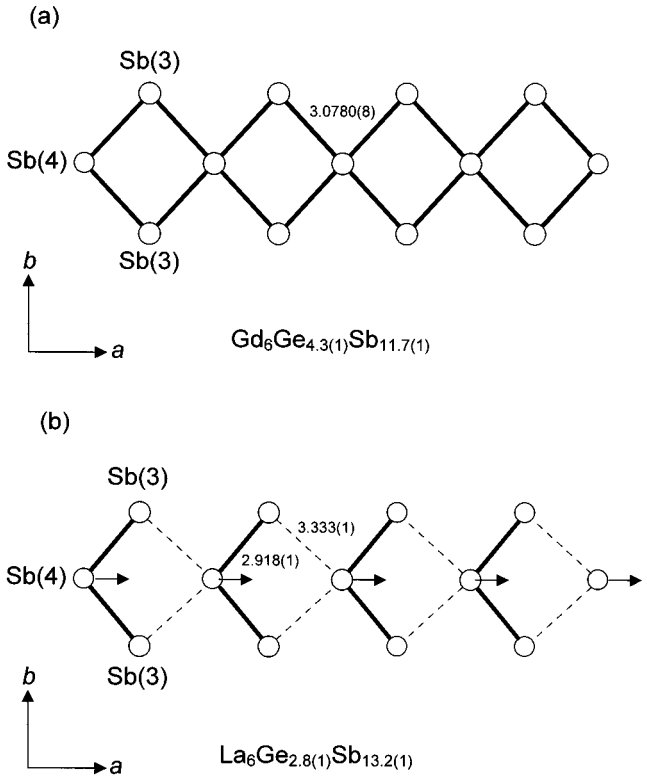

Figure 4. Comparison of the symmetrical and asymmetrical three-atom-wide Sb ribbons, built up of Sb(3) and Sb(4), in (a) $Gd_6Ge_{4.3(1)}Sb_{11.7(1)}$ and (b) $La_6Ge_{2.8(1)}Sb_{13.2(1)}$, respectively, as viewed perpendicular to the plane of the strips.

Figure 4 for the $Gd_6Ge_{4.3(1)}Sb_{11.7(1)}$ and $La_6Ge_{2.8(1)}Sb_{13.2(1)}$ members. In $Gd_6Ge_{4.3(1)}Sb_{11.7(1)}$, the symmetrically organized strips consist of Sb(4) atoms that reside at the center ($^1/_2$, $^1/_2$, 0) of the squares outlined by Sb(3) atoms, yielding four equivalent Sb(3)−Sb(4) distances of 3.0780(8) Å (Figure 4a). These Sb−Sb distances have been postulated to correspond to one-electron half-bonds[2,3,26−29] which are ubiquitous in Sb square sheets, such as those observed in $LaSb_2$ (3.087−3.157 Å),[30] $LaIn_{0.8}Sb_2$ (3.119(3)−3.142(3) Å),[2] and $LaZn_{0.52}Sb_2$ (3.097(2) Å).[31] A useful interpretation of these ribbons is to consider them to be excised from infinite square nets.[32] Using this analogy, one can envisage Sb ribbons or strips of varying atom widths (n) ranging from linear skewers ($n = 1$) and zigzag chains ($n = 2$) to increasingly wider ribbons ($n = 6$ or greater); we have now identified many structures containing these ribbons.[1,26,32−34] In $La_6Ge_{2.8(1)}Sb_{13.2(1)}$, the central Sb(4) atoms in the ribbons are located asymmetrically off-center (∼0.43, $^1/_2$, 0), creating two closely spaced symmetry-equivalent sites about a mirror plane, only one of which can be occupied locally. One way to view such a picture is in terms of an energetically favorable second-order Peierls-type sliding distortion of the symmetrical ribbon, as observed in the related alloy La_6MnSb_{15}.[20] A distortion along a, such as that shown in Figure 4b, necessarily results in alternating short (2.918(1) Å) and long (3.333(1) Å) Sb(3)−Sb(4) distances. For comparison, intralayer Sb−Sb single-bond lengths of 2.908 Å and weaker interlayer interactions of 3.355 Å are observed in elemental Sb.[35] A similar situation exists for the three-atom-wide ribbons in $Nd_6Ge_{3.6(1)}Sb_{12.4(1)}$, where the short and long Sb(3)−Sb(4) distances are 2.9175(9) and 3.279-(1) Å, respectively. One can rationalize that the distortion should occur more prominently in structures containing the largest *RE* components, viz., $La_6Ge_{2.8(1)}Sb_{13.2(1)}$, because the cell expansion would force a symmetrical ribbon to have four longer and therefore weaker Sb−Sb bonds. The asymmetric distortion optimizes stability by allowing two full Sb−Sb single bonds to form at the expense of the two weakened Sb−Sb interactions within a Sb(4)−Sb(3)−Sb(4)−Sb(3) square. This is consistent with the similarity in the short Sb(3)−Sb(4) distances in the La and Nd compounds, despite the significant reduction in cell volume due to lanthanide contraction. The reduced cell volume of the Gd compound favors a more symmetrical ribbon by formation of four half-bonds as opposed to the proposed alternative configuration. It should be appreciated that the interpretation of these Sb−Sb contacts as half-bonds is a simplification, given that there exists a continuum of Sb−Sb distances in this intermediate range of values.

The decomposed view (Figure 3b) of the structure also reveals kinked sheets parallel to b, derived from folding an idealized

(26) Ferguson, M. J.; Hushagen, R. W.; Mar, A. *J. Alloys Compd.* **1997**, *249*, 191.
(27) Brylak, M.; Möller, M. H.; Jeitschko, W. *J. Solid State Chem.* **1995**, *115*, 305.
(28) Brylak, M.; Jeitschko, W. *Z. Naturforsch., B: Chem. Sci.* **1994**, *49*, 747.
(29) Nesper, R. *Prog. Solid State Chem.* **1990**, *20*, 1.
(30) Wang, R.; Steinfink, H. *Inorg. Chem.* **1967**, *6*, 1685.
(31) Cordier, G.; Schäfer, H.; Woll, P. *Z. Naturforsch., B: Anorg. Chem., Org. Chem.* **1985**, *40*, 1097.
(32) Lam, R.; Mar, A. *Inorg. Chem.* **1998**, *37*, 5364.
(33) Lam, R.; Mar, A. *Inorg. Chem.* **1996**, *35*, 6959.
(34) Bolloré, G.; Ferguson, M. J.; Hushagen, R. W.; Mar, A. *Chem. Mater.* **1995**, *7*, 2229.
(35) Donohue, J. *The Structures of the Elements*; Wiley: New York, 1974.

square net at every fifth atom. The resulting folded sheets consist of six-atom-wide sections (Sb(5)−Sb(6)−Sb(2)−Sb(2)−Sb(6)−Sb(5)) which are approximately parallel to (011) and (0$\bar{1}$1). A consequence of the acute angles (∼48°), subtended by Sb(6)−Sb(5)−Sb(6), which form at the corners of the bends is short distances (2.547(2)−2.615(2) Å) between Sb(6) atoms from adjacent sections, unreasonably short to be Sb−Sb bonds but ideal for Ge−Sb or Ge−Ge bonds. These distances may be compared to Ge−Ge single-bond distances in the clathrate $Cs_8Na_{16}Ge_{136}$ (2.4859(7)−2.5033(9) Å)[36] or elemental Ge (2.4497(1) Å).[35] Somewhat more rare are clear examples of Ge−Sb bond distances in the literature. If we accept values of 2.62 Å, the bond valence parameter for a Ge−Sb single bond,[37] or 2.66(2)−2.68(2) Å, observed in the disordered clathrate $Ge_{14}(GaSb)_{12}Sb_8I_8$,[38] as reasonable Ge−Sb single-bond distances, then a possible explanation for the inherent disorder actually observed at this site is that Sb−Sb repulsions are eliminated in favor of reasonable Ge−Sb and Ge−Ge bonding interactions through incorporation of Ge into this site. In $La_6Ge_{2.8(1)}Sb_{13.2(1)}$, the M(1)−M(1) distance of 2.615(2) Å represents an ideal Ge−Sb single-bond distance. The observed Ge(1):Sb(6) ratio of 61(3):39(2) is consistent with a hypothesized local environment of mostly Ge−Sb single bonds, with weaker Ge−Ge contacts substituted occasionally. Substituting La with smaller *RE* atoms results in reduced M(1)−M(1) distances of 2.588(1) Å (*RE* = Nd) and 2.547(2) Å (*RE* = Gd). These values become increasingly too short for Ge−Sb bonds but converge to ideal Ge−Ge single bond distances. Thus, consistent with the predicted trend of increasing number of Ge−Ge bonds as the M(1)−M(1) distance decreases are the observed larger amounts of Ge(1) relative to Sb(6) for $Nd_6Ge_{3.6(1)}Sb_{12.4(1)}$ (72(3)%) and $Gd_6Ge_{4.3(1)}Sb_{11.7(1)}$ (83(3)%). The implication of some unusually short Ge−Sb contacts (2.547(2)−2.588(1) Å), randomly distributed throughout the extended network, is intriguing.

A view perpendicular to one of the six-atom-wide sections making up the kinked sheets is shown in Figure 5. A pattern of long−short−long−short−long for the interatomic distances is apparent in the square nets. For the Gd compound, in which the M(1) site contains mostly Ge, the section is best viewed (Figure 5a) as four-atom-wide ribbons, where the Ge−Sb and Sb−Sb bonds within are fractional in bond order. In the structure of the La compound, in which the M(1) site consists of almost equal proportions of Ge and Sb, the square net (Figure 5b) is best interpreted as weakly associating zigzag chains.

The overall structure of $RE_6Ge_{5-x}Sb_{11+x}$ can now be appreciated by recondensing these artificially separated subunits to form the real structure. Stacking the kinked sheets along [001] with the Sb(5) corners approaching each other sees the emergence of large channels defined by the six-atom-wide ribbons discussed earlier. By reintroduction into each channel of two columns of Sb(1)-centered trigonal prisms of *RE* atoms and a three-atom-wide Sb ribbon, a "hole" centering on position (0, 0, 0) is generated at the junction. The actual three-dimensional structure can now be obtained by filling sites (0, ∼0, 0) (M(2)) residing slightly off-center with Ge(2) and Sb(7) atoms which link together the kinked sheets and ribbons to form an overall extended network.

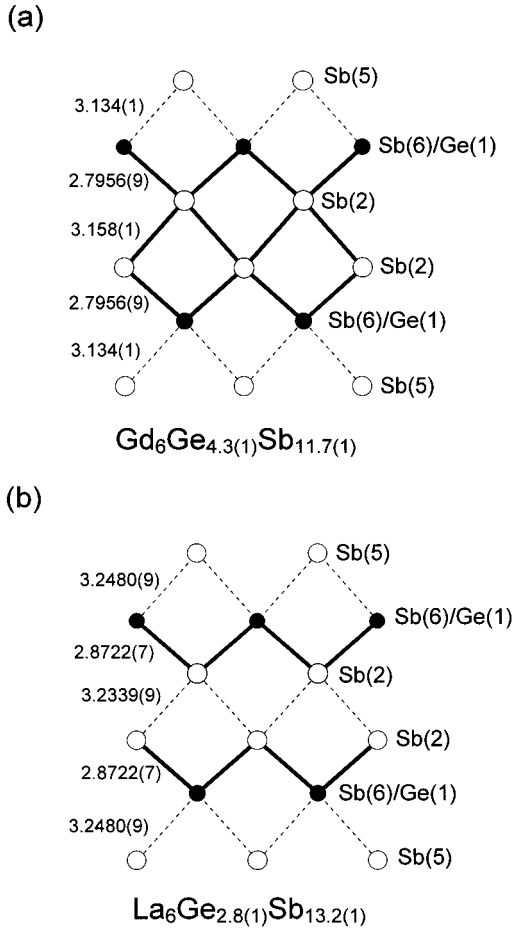

Figure 5. Comparison of the six-atom-wide sections making up the kinked sheets in (a) $Gd_6Ge_{4.3(1)}Sb_{11.7(1)}$ and (b) $La_6Ge_{2.8(1)}Sb_{13.2(1)}$, respectively, as viewed perpendicular to the plane of the atoms. On the basis of bond distances and atomic distributions in the M(1) site, local interpretations of four-atom-wide ribbons (*RE* = Gd) and zigzag chains (*RE* = La) are emphasized for the six-atom-wide sections. Thick lines represent bond orders greater than 0.5, and dashed lines represent weak bonding interactions.

Since M(2) is less than 1 Å away from a symmetry-equivalent position across a mirror plane in the three crystal structures, the maximum occupancy is 50%, or put another way, only one of these can be occupied locally. The Ge(2) content at this disordered site increases dramatically from the La (19(2)%) to the Nd (36(2)%) compound. In $Gd_6Ge_{4.3(1)}Sb_{11.7(1)}$, this site is no longer disordered, being occupied (at 50%) instead exclusively by Ge(2). The increase in Ge content at M(2) may be explained by examining the distances to neighboring atoms. The coordination geometry of the M(2) position is a square pyramid, as outlined by four Sb(5) atoms defining the square base and one Sb(3) atom forming the apex. In $La_6Ge_{2.8(1)}Sb_{13.2(1)}$, the distances from M(2) to Sb(5) (2.9320(8) Å) and Sb(3) (2.743(2) Å) represent ideal separations for Sb−Sb bonds. Despite the fact that the latter distance (M(2)−Sb(3)) also falls within favorable Ge−Sb bonding interactions, the stronger Sb−Sb orbital overlaps may be the reason for the relatively higher proportion of Sb(7) compared to Ge(2) observed for this site. In $Gd_6Ge_{4.3(1)}Sb_{11.7(1)}$, both distances are notably reduced, yielding Ge(2)−Sb(5) and Ge(2)−Sb(3) separations of 2.781(1) and 2.709(5) Å, respectively. Although unusually short Sb−Sb single-bond distances have been reported for the compounds $[C_{18}H_{36}N_2O_6{\cdot}Na]_3[Sb_7]$ (2.693(4) Å),[39] NdPdSb (2.709(1) Å),[40] $NbSb_2$ (2.711 Å),[41,42] $[K(2,2,2\text{-crypt})]_3[Sb_7]$ (2.717(2) Å),[43] and

(36) Bobev, S.; Sevov, S. C. *J. Am. Chem. Soc.* **1999**, *121*, 3795.
(37) O'Keeffe, M.; Brese, N. E. *Acta Crystallogr., Sect. B: Struct. Sci.* **1992**, *48*, 152.
(38) von Schnering, H. G.; Menke, H. *Z. Anorg. Allg. Chem.* **1976**, *424*, 108.

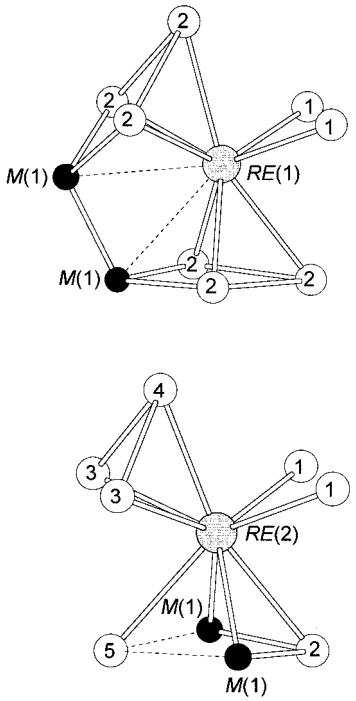

Figure 6. Coordination environments around the *RE*(1) and *RE*(2) atoms, showing bicapped-trigonal-prism and monocapped-square-antiprism geometries, respectively. Alternatively, the coordination of *RE*(1) may be described as a bicapped square antiprism if the two M(1) atoms, situated further away as shown by the dashed lines, are considered.

$[Na(2,2,2\text{-crypt})]_3[Sb_{11}]$ (2.716(4) Å)[44] with values around 2.75 Å more common in other examples,[45−47] the relatively high coordination number surrounding this site in the Gd compound would be sterically unfavorable for any Sb occupancy. Interestingly, the middle member $Nd_6Ge_{3.6(1)}Sb_{12.4(1)}$ exhibits values of 2.8434(6) and 2.653(2) Å for distances to the basal and apical atoms, respectively. Despite the short M(2)−Sb(3) separation, Sb is still present at this site at 14(1)% occupancy. Comparison may be made to the organometallic complexes $[Sb\{C_6H_2[CH(SiMe_3)_2]_3\text{-}2,4,6\}]_2$,[48] $[Sb(C_6H_3Mes_2\text{-}2,6)]_2$ (Mes = C_6H_2−2,4,6-Me_3),[49] and $[Sb(C_6H_3Trip_2\text{-}2,6)]_2$ (Trip = C_6H_2−2,4,6-$^iPr_3$)[49] where multiple-bond character[50,51] has been invoked to explain the short Sb−Sb separations (2.642(1)−2.668(2) Å). Caution should be exercised here, however, because the observed M(2)−Sb(3) distance of 2.653(2) Å may be artificially shortened by the disorder modeling in structure refinements. It should be expected that the equilibrium positions of Ge(2) and Sb(7) will be independently achieved locally in the structure. The nonspherical displacement parameters for this site in all three compounds are supportive of this fact.

(39) Adolphson, D. G.; Corbett, J. D.; Merryman, D. J. *J. Am. Chem. Soc.* **1976**, *98*, 7234.
(40) Mehta, A.; Malik, S. K.; Yelon, W. B. *J. Magn. Magn. Mater.* **1995**, *147*, 309.
(41) Furuseth, S.; Kjekshus, A. *Nature* **1964**, *203*, 512.
(42) Furuseth, S.; Kjekshus, A. *Acta Crystallogr.* **1965**, *18*, 320.
(43) Critchlow, S. C.; Corbett, J. D. *Inorg. Chem.* **1984**, *23*, 770.
(44) Bolle, U.; Tremel, W. *J. Chem. Soc., Chem. Commun.* **1992**, 91.
(45) Cordier, G.; Ochmann, H. *Z. Kristallogr.* **1991**, *197*, 297.
(46) Shreeve-Keyer, J. L.; Haushalter, R. C.; Seo, D.-K.; Whangbo, M.-H. *J. Solid State Chem.* **1996**, *122*, 239.
(47) Asbrand, M.; Eisenmann, B. *Z. Kristallogr.* **1992**, *198*, 309.
(48) Tokitoh, N.; Arai, Y.; Sasamori, T.; Okazaki, R.; Nagase, S.; Uekusa, H.; Ohashi, Y. *J. Am. Chem. Soc.* **1998**, *120*, 433.
(49) Tramley, B.; Sofield, C. D.; Olmstead, M. M.; Power, P. P. *J. Am. Chem. Soc.* **1999**, *121*, 3357.
(50) Power, P. P. *J. Chem. Soc., Dalton Trans.* **1998**, *2939*.
(51) Power, P. P. *Chem. Rev.* **1999**, *99*, 3463.

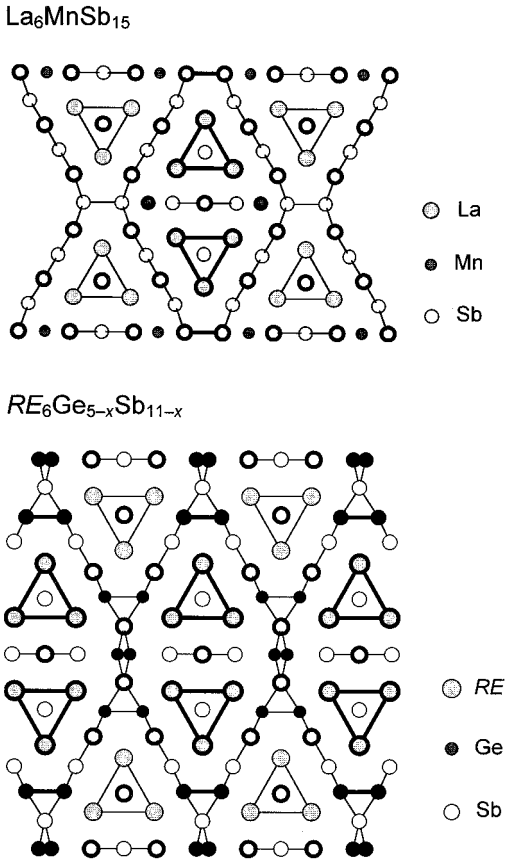

Figure 7. Comparison of the structures of (a) La_6MnSb_{15} and (b) $RE_6Ge_{5-x}Sb_{11+x}$ shown in projection down the shortest axis. Circles with thicker rims are atoms residing in planes displaced by $^1/_2$ the short axis parameter.

As shown in Figure 6, the coordination environments around *RE*(1) (CN 8) and *RE*(2) (CN 9) are representative of a bicapped trigonal prism and a monocapped square antiprism, respectively. In the first type of arrangement, two Sb(1) and four Sb(2) atoms define the trigonal prism. Additional Sb(2) atoms then cap two of the rectangular faces to form the bicapped trigonal prism. If the two nearby M(1) atoms, at much longer distances away, are considered, then the geometry may be described as a bicapped square antiprism where one M(1) atom caps a trigonal face while an Sb(2) atom caps a square face. The second environment, adopted by *RE*(2), is more reminiscent of the type of coordination geometry observed for the rare-earth atoms in other solid-state compounds of the main-group elements,[2,3] where two-dimensional square nets are common. The monocapped square antiprism adopted by *RE*(2) is outlined by a basal square consisting of the combination Sb(5)−M(1)−Sb(2)−M(1), another square, twisted 45° relative to the first, defined by two each of the Sb(1) and Sb(3) atoms, and a capping Sb(4) atom. The *RE*−Sb and *RE*−Ge distances (Table 5) in the three structures are comparable to those found in binary rare-earth antimonide and germanide compounds.

Structural Relationships. There exists a large family of structures based on the stacking of trigonal prisms whose vertexes are metal atoms. If attention is drawn to the columns of face-sharing trigonal prisms of *RE* atoms in $RE_6Ge_{5-x}Sb_{11+x}$, then a structural connection can be made to the compound La_6MnSb_{15},[20] as shown in Figure 7. For purposes of comparison, the two structures are best viewed in terms of the six-sided large channels which are clearly outlined in La_6MnSb_{15} by two- and six-atom-wide segments of Sb atoms, together making up the 22-membered circumference. If each channel shares its six sides

with adjacent channels to create a perfect fit, then the structure of La_6MnSb_{15} is obtained. In $RE_6Ge_{5-x}Sb_{11+x}$, each channel shares only four atoms from the six-atom sections with adjacent channels, resulting in a nonideal packing of the channels. The corners where the six-atom sections meet necessarily must cross with those from neighboring channels using this mode of packing, creating the short M(2)−M(2) distances.

In conclusion, a new series of rare-earth germanium antimonides was synthesized and structurally characterized. The novel structure illustrates the importance of contributions of strong as well as weak homoatomic bonding between the main-group elements toward the overall stability of extended structures. As in the corresponding Ga system,[1] it may be worthwhile targeting related structures forming part of a homologous series. Interesting properties may be expected to arise from the triangular arrangements of the *RE* atoms forming columns of trigonal prisms. The results of resistivity and magnetic measurements of the series are reported separately.[11]

Acknowledgment. This work was supported by the Natural Sciences and Engineering Research Council of Canada and the University of Alberta. We thank Christina Barker (Department of Chemical and Materials Engineering) for assistance with the EDX analyses. Helpful discussions with Prof. F. W. B. Einstein (Simon Fraser University) regarding the structure determinations are gratefully acknowledged.

Supporting Information Available: Listings of powder X-ray diffraction data for $RE_6Ge_{5-x}Sb_{11+x}$ (RE = La−Nd, Sm, Gd−Dy) and tables of further crystallographic details, along with one consolidated X-ray crystallographic file (for three structures), in CIF format. This material is available free of charge via the Internet at http://pubs.acs.org.

IC0009472